

***Weak-Link Mechanisms  
for Ultraprecision Synchrotron Radiation Instruments  
at the Advanced Photon Source***

***D. Shu, T. S. Toellner, E. E. Alp, J. Maser, J. Ilavsky, S. D. Shastri,  
P. L. Lee, S. Narayanan, and G. G. Long***

***Advanced Photon Source  
Argonne National Laboratory  
Argonne, Illinois 60439, U.S.A.***

***MEDSI/SRI-2008, Saskatoon, Canada***

***June 12, 2008***



UChicago  
Argonne, LLC

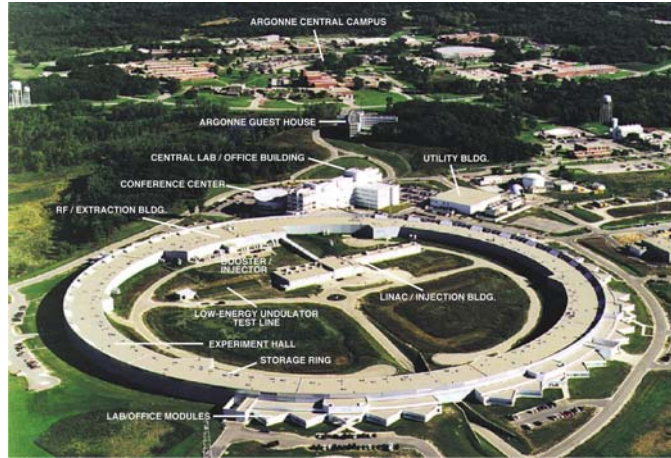


A U.S. Department of Energy laboratory  
managed by UChicago Argonne, LLC

## **Outline**

- **Introduction**
- **Rotary laminar weak-link mechanism**
  - *New high-energy-resolution monochromator for high-resolution inelastic x-ray scattering applications*
  - *High-resolution crystal analyzer for ultra-small-angle x-ray scattering instrument*
  - *High-resolution crystal analyzer array for x-ray powder-diffraction instrument*
- **UHV compatible rotary laminar weak-link mechanism**
  - *UHV-compatible artificial channel-cut crystal monochromator for XPCS applications*
  - *UHV-compatible artificial channel-cut crystal monochromator for high pressure research*
- **Linear laminar weak-link mechanism**
  - *Laminar weak-link stages for x-ray scanning nanoprobe*
- **Summary**

## Introduction



The Advanced Photon Source (APS) at the Argonne National Laboratory is a national user facility for synchrotron radiation research.

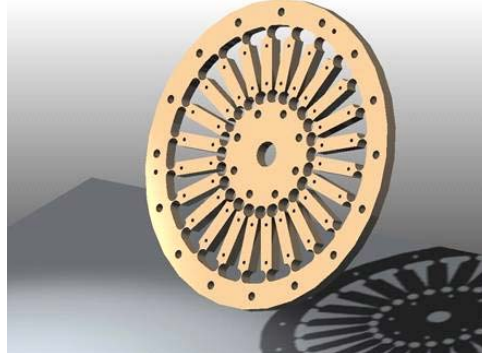
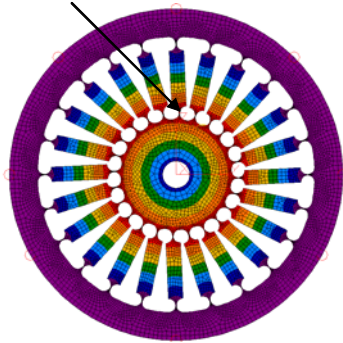
## Introduction

● In 1999, to overcome the obstacles in developing a 4-crystal in-line high-resolution hard x-ray monochromator using a nested channel-cut crystal geometry with meV bandpass [1], the first high-stiffness weak-link mechanism with stacked thin-metal sheets was developed [2] for the Advanced Photon Source (APS) high-energy-resolution beamline 3-ID [3]. The precision and stability of this mechanism allowed us to align or adjust an assembly of crystals to achieve the same performance as does a single channel-cut crystal, so we called it an "artificial channel-cut crystal." Using this mechanism, we can make an outer channel-cut crystal large enough to optimize the nested monochromator's performance and compensate the crystal local temperature and strain variations. A **less-than-25-nrad-per-hour angular drift** of two crystals was demonstrated in a two-hour stability test with a **1-meV bandwidth** monochromatic beam [2].

● Since then, more than **forty sets** of such rotary weak-link mechanisms have been made for APS users in applications, such as high-energy-resolution monochromators for inelastic x-ray scattering and x-ray analyzers for ultra-small-angle scattering and powder-diffraction experiments. Their typical angular positioning resolution is **20-40 nrad** with a travel range of **up to 1.2 degrees**.

### Weak-link mechanism for high-energy-resolution x-ray monochromator

maximum displacement 94  $\mu\text{m}$  with maximum von Mises stress 175 MPa



Left: A finite-element simulation for a wheel-shaped rotary weak-link module. It shows the displacement distribution under a 0.89 Nm torsion load on the center part while the outer ring is fixed on the base.

Right: A 3-D model of a typical overconstrained rotary weak-link module. It consists of 16 layers of stainless-steel weak-link sheets bonded together with a total thickness of 4 mm.

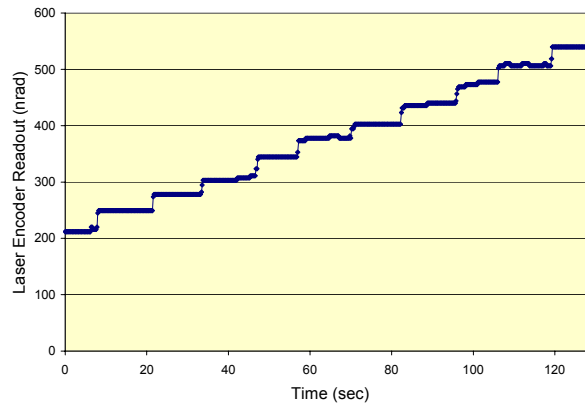
### Weak-link mechanism for high-energy-resolution x-ray monochromator



A novel miniature overconstrained weak-link mechanism that allows positioning of two crystals with better than 30-nrad angular resolution has been developed at the APS [8,9]. The precision and stability of this structure allow the user to align or adjust an assembly of crystals to achieve the same performance as a single channel-cut crystal, so we call it an "artificial channel-cut crystal."

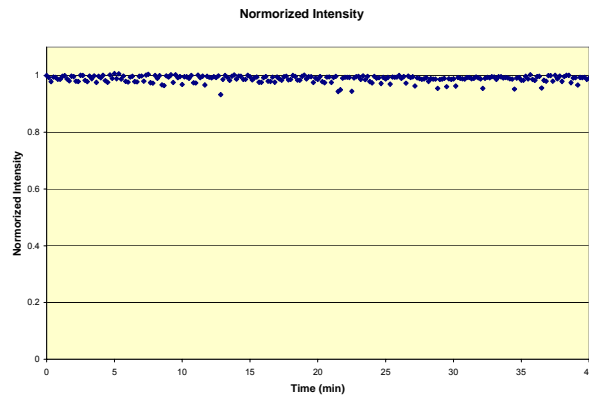
**Weak-link mechanism for high-energy-resolution x-ray monochromator at APS XOR 3-ID-B**

- Sensitivity test with a laser Doppler encoder  
A test with 33 nrad average step size



**Weak-link mechanism for high-energy-resolution x-ray monochromator at APS XOR 3-ID-B**

- Stability result from a x-ray experiment  
Relative intensity measured by an ionization chamber after the high-resolution monochromator (1-meV bandwidth) as a function of time. The data are corrected for the decaying current in the storage ring.



### **Weak-link mechanism for high-energy-resolution x-ray monochromator**



The availability of this novel mechanism makes life easier for novel x-ray crystal optics developers, because of the possibility of free-to-use asymmetric-cut crystals in the monochromator design to improve angular acceptance and energy resolution. It also provides the capability to perform a dynamic angular adjustment for temperature compensation between two crystals.

### **Weak-link mechanism for high-energy-resolution x-ray monochromator at APS XOR 3-ID-B**

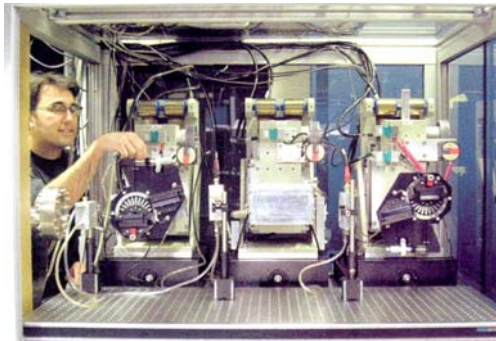


Figure shows APS staff scientist Tom Toellner at the new monochromator used for HRIXS. The cryogenically cooled, high-resolution monochromator transmits a 1.2-meV-bandwidth x-ray beam with 60% spectral efficiency.

The first pair and last pair of reflections are aligned to the silicon (2 2 0) crystal reflection with special crystal surfaces cut for matching of the reflection width of the middle pair of the cryogenically cooled silicon (15 11 3) crystal reflection. Laminar weak-link mechanisms are utilized for alignment of the first pair and last pair crystals\*.

\*T. S. Toellner, APS Science 2004, ANL-05/04, p. 130

### Weak-link mechanism for high-energy-resolution x-ray monochromator at APS Sector 33



Sine-bar with PZT

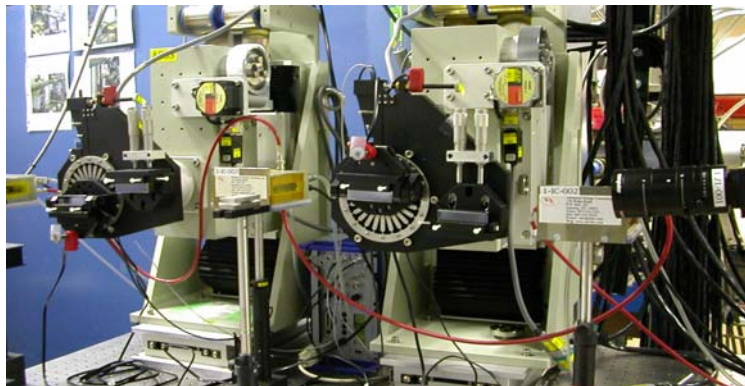
The applications were also expanded to the high-resolution crystal analyzer and the analyzer array for x-ray powder diffraction instrumentation. Figure shows a rotational stage using an overconstrained weak-link mechanism for the National Institute of Standards and Technology's (NIST) ultra-small-angle x-ray scattering instrument at the APS UNICAT sector 33 experimental station.

DC-motor actuator

Weak-link mechanism

Crystal analyzer

### Weak-link mechanism for high-energy x-ray monochromator at APS 1-ID-B



Photograph of a high-energy x-ray monochromator with four crystal reflections constructed at APS XOR beamline 1-ID-B. It shows a high-energy (50-100 keV) high-resolution x-ray monochromator with four crystal reflections constructed at APS beamline 1-ID-B, which has been used for resonant powder diffraction\* and stress/strain studies\*\*.

\* Y. Zhang, A. P. Wilkinson, P. L. Lee, S. D. Shastri, D. Shu, D. -Y. Chung, M. G. Kanatzidis, J. Appl. Cryst. 38, 433-441 (2005).

\*\* B. Jakobsen, H. F. Poulsen, U. Lienert, J. Almer, S. D. Shastri, H. Sorensen, C. Gundlach, W. Pantleon, Science 312, 889-892 (2006).

### Weak-link mechanism for an x-ray powder diffraction instrument at APS XOR sector 11

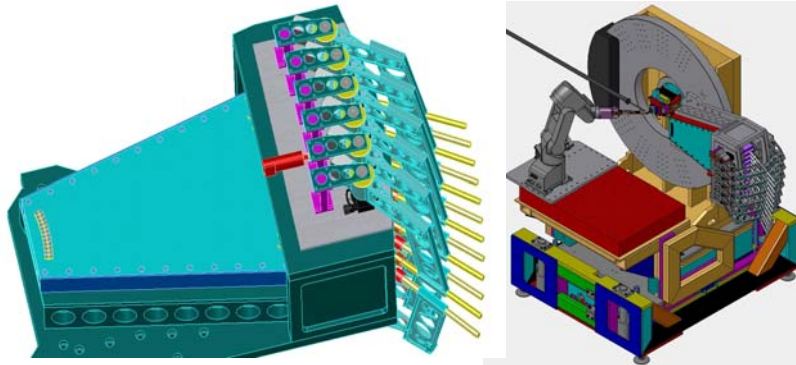
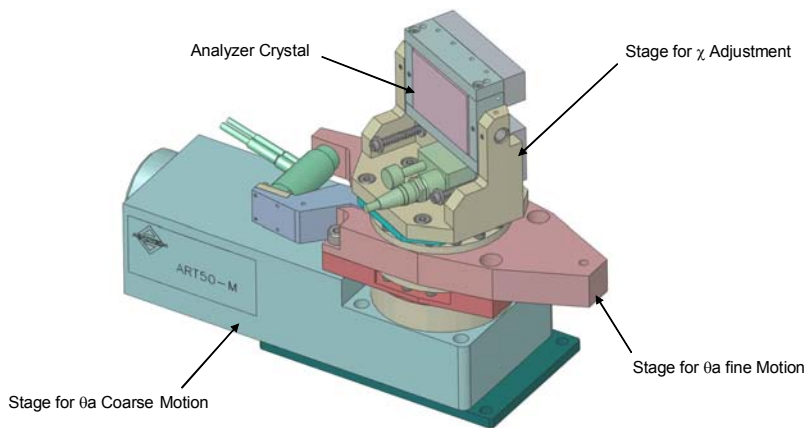


Figure shows a 3-D model of the analyzer array for an x-ray powder diffraction instrument at APS XOR sector 11. There are twelve silicon (1 1 1) or germanium (2 2 0) crystal analyzers in this array, each of them includes a PZT-driven laminar weak-link mechanism for the crystal's fine pitch adjustment with a resolution of better than 0.05 arc-sec\*.

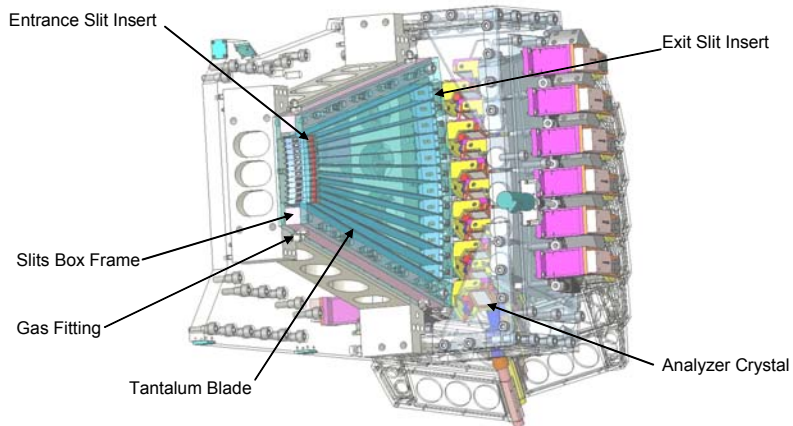
\* P. Lee, M. A. Beno, D. Shu, M. Ramanathan, J. F. Mitchell, J. D. Jorgensen, and R. B. Von Dreele, SRI 2003 Conf. Proc. 705, AIP (2004) 388-391.

### Stages for high-resolution crystal analyzer



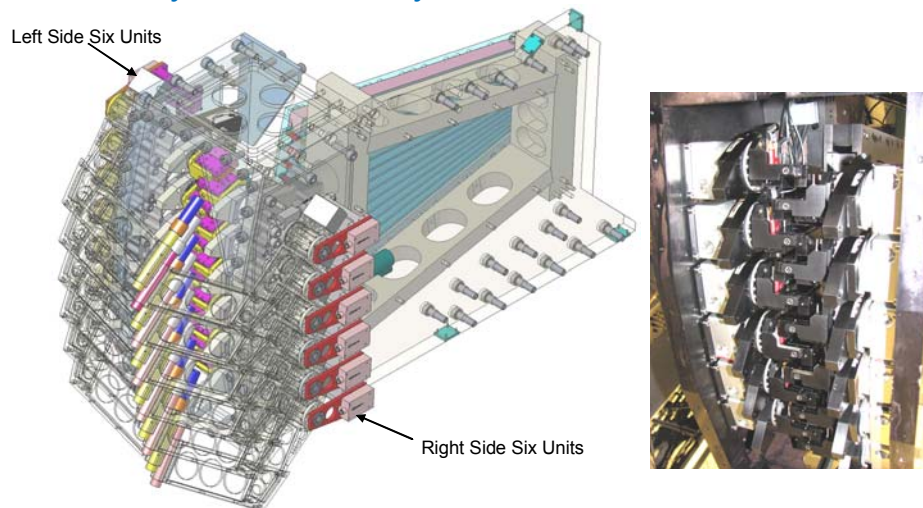
For each of the analyzer crystals, there are three positioning devices stacked together to control the crystal's angle  $\theta_a$  coarse motion, angle  $\theta_a$  fine motion, and angle  $\chi$  adjustment. A commercial rotary stage ART-50 from Aerotech™ Inc. U.S.A. is applied for the analyzer crystal's angle  $\theta_a$  coarse positioning.

### *X-ray slits array*



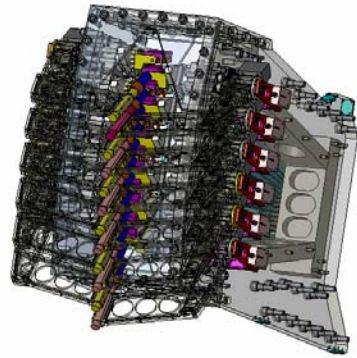
The slits box consists of an aluminum slits box frame, tantalum x-ray insulating blades, and 24 slit inserts. The slit inserts are precisely exchangeable. A set of slit inserts is manufactured to cover the tantalum knife-edge slit size range from 0.2 mm to 3 mm for various applications.

### *Twelve-analyzer and detector system*

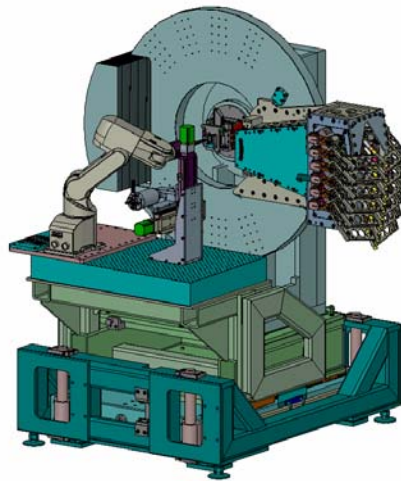


We grouped the twelve analyzers and detectors into two sub-assemblies: left side six units and right side six units.

*Twelve-analyzer and detector system*

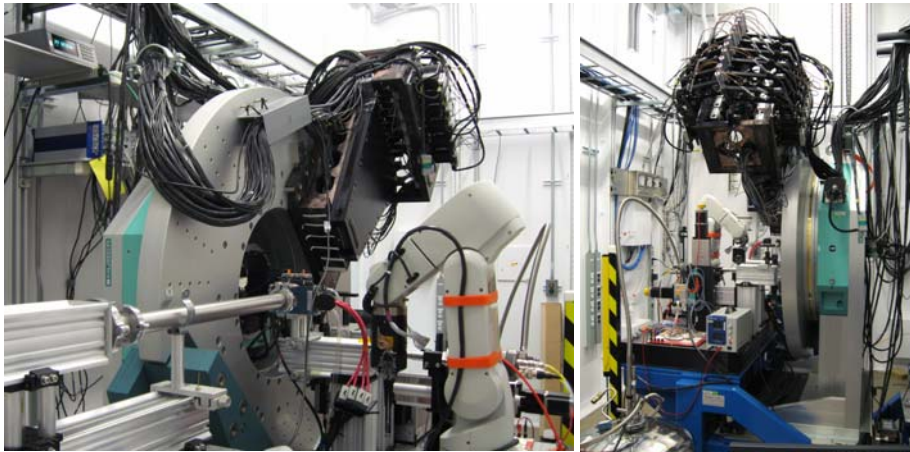


*General layout*



A 3-D model of the high-resolution diffractometer with 12-analyzer/detector system

### *General layout*



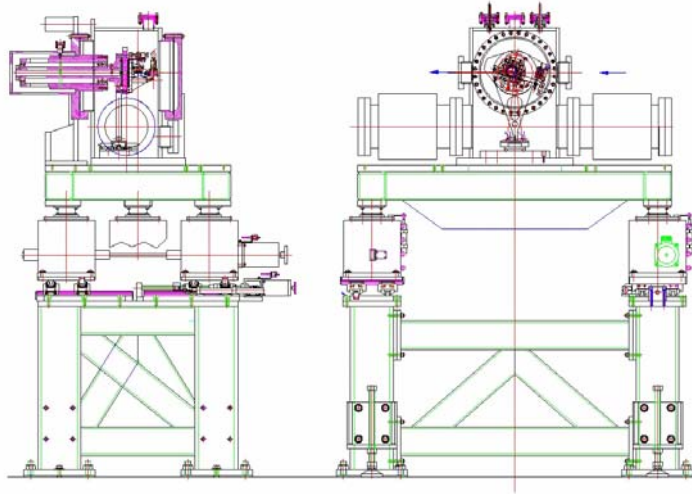
The high-resolution diffractometer has a dimension of 2600 mm (H) X 2100 mm (L) X 1700 mm (W). The main circle of the goniometer has a vertical mounting disk with an outside diameter of 1200 mm.

### *In-vacuum weak-link positioning devices design*

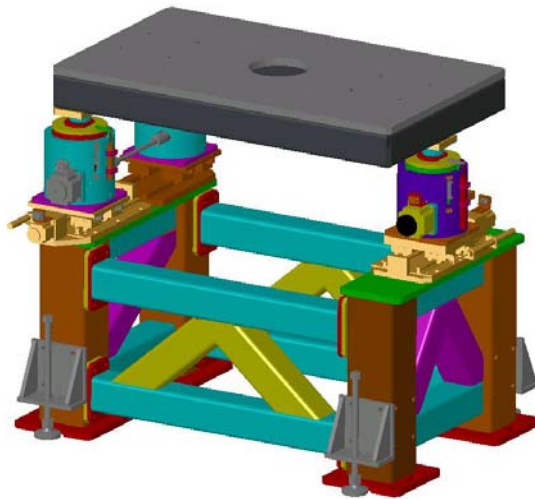
Many synchrotron radiation instruments require high-vacuum (HV) or ultra-high-vacuum (UHV) compatibility. Special design practices need to be established for the HV- or UHV-compatible device to minimize the gas load and maximize the pumping speed. The major design considerations for an HV-or-UHV-compatible device include:

- Selecting the HV- or UHV-compatible material with which to construct the device
- Minimizing the device surface area open to vacuum
- Eliminating any trapped volumes in the device and component design
- Selecting the proper surface quality and manufacturing process
- Compatibility with cleaning process and bake temperature
- Selecting the proper material for friction pair
- Selecting the proper cooling method
- Mechanical stabilizing under vacuum force

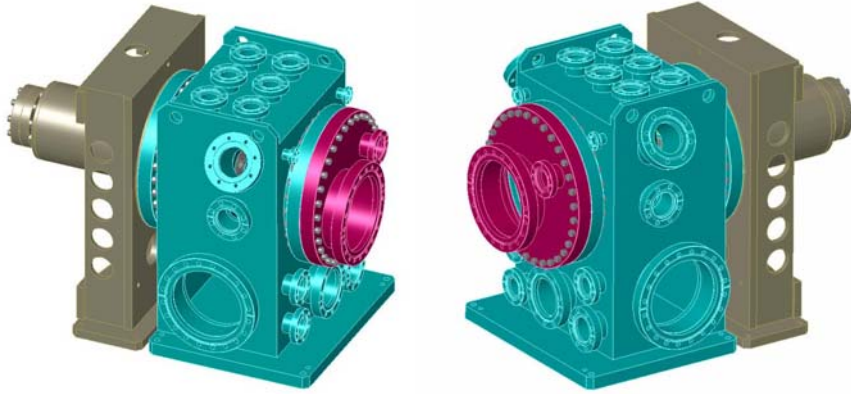
*Weak-link mechanism for UHV Monochromator at APS XOR 8-ID  
for x-ray photon correlation spectroscopy applications*



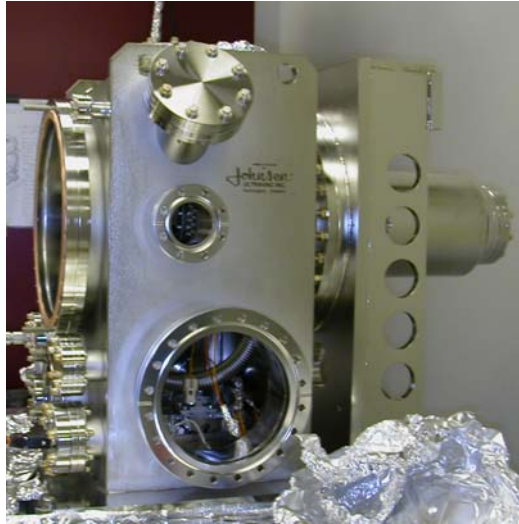
*Monochromator Supporting Structure*



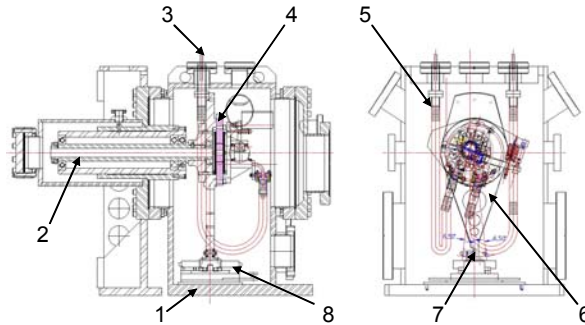
*Monochromator Vacuum Tank*



*Monochromator Vacuum Tank*



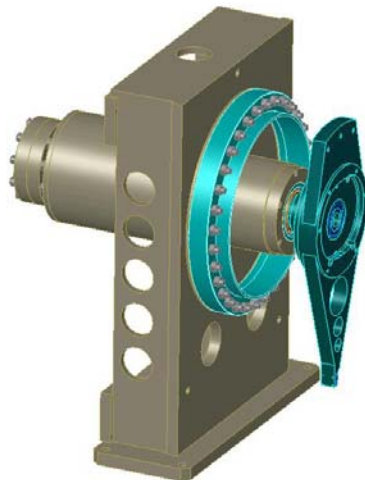
### Monochromator Sine Bar Structure and Driver



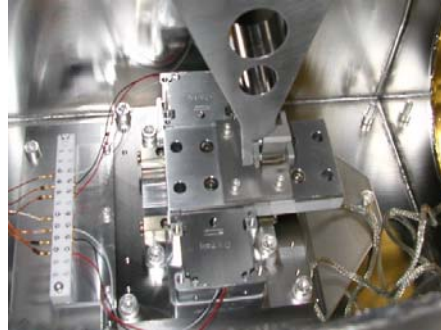
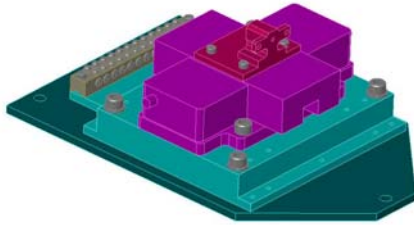
Detailed cross-sectional side and front views showing the mechanical and vacuum design of the artificial channel cut monochromator. In the center and right panels the "pink" x-ray beam is incident from the right and the monochromatic beam is transmitted to the left.

Referring to this figure, a precision hollow shaft (2) supported by two sets of shaft bearings inside a precisely machined rigid housing permits stable angular rotation of the crystal by means of the sine-bar mechanism. The sine bar (6) is mounted to the shaft (2) with maximized rigidity, permitting the 236-mm-long sine bar to have a  $13^\circ$  rotation range. Using a hardened ruby ball (7) as a precision contact point, the sine-bar arm is driven by a commercial UHV-compatible ceramic-motor-driven linear positioning stage (8) that has 10 nanometer closed-loop linear resolution based on an UHV-compatible linear grating encoder on the stage [5], yielding high angular resolution (42 nrad, theoretically) of the artificial channel-cut assembly. The artificial channel-cut crystal mechanism (4) is attached to front of the sine bar, which is cradled with the high-stiffness precision shaft. The entire assembly, including the channel-cut crystal cage (see below), is contained in a compact UHV vacuum chamber (1) eliminating the use of bellows to transmit the motion and thereby any residual vacuum forces. Water cooling is provided by bellows-insulated cooling lines (3, 5). [8]

### Monochromator Sine Bar Structure and Driver



## Monochromator Sine Bar Structure and Driver

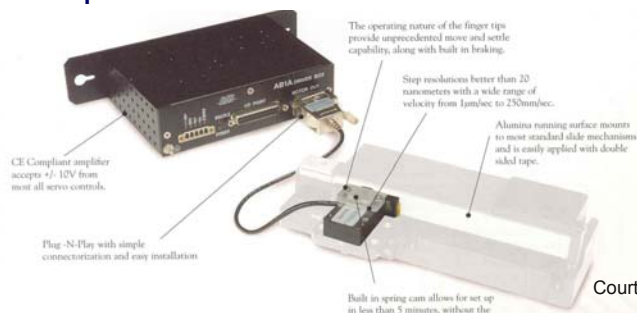


Achieving the mechanical and vacuum design requirements required incorporation of several novel UHV-compatible motion stages. Chief among them is an UHV-compatible linear slide assembly comprised of a precision slide from Alio Industries™, piezoelectric actuators from Nanomotion™, an encoder from Renishaw™, and an ACS Motion™ SPiiPlus stand-alone Ethernet servo controller. The combination delivers exceptionally precise closed-loop positioning in vacuum over extended length scales and velocity ranges. [8]

## Monochromator Sine Bar Structure and Driver

### Nanomotion™ piezoelectric motor

- Based on the principles of ultrasonic standing waves in piezoelectricity
- Operating similarly to DC servo motors with high resolution
- Closed-Loop feedback with a grating encoder
- UHV-Compatible



Courtesy of Nanomotion Inc.

## Monochromator Sine Bar Structure and Driver

### HR Series

Nanomotion's HR Series motors range in size from a single element (providing 4N of force) to an eight element motor (providing 32N of force). The HR series is capable of driving both linear and rotary stages at a wide dynamic range of speed, from several microns per second to 250mm/sec and can easily mount to traditional low friction stages or other devices. The unique operating characteristics of the HR Series motors provide inherent braking and the ability to eliminate servo jitter when in a static position.

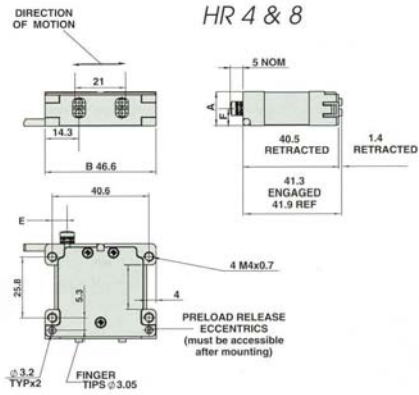
### Features

- Unlimited Travel
- Wide Dynamic Velocity Range
  - From 1µm/sec to 250mm/sec
- Excellent Allow & Hold
- Step Resolutions to 5µm
- No Intrinsic Magnetic Field
- No External Magnetic Field Sensitivity (for Non-Magnetic Version)
- Vacuum Versions Available

### Motor Performance Specifications

Model	Max Velocity (mm/sec)	Dynamic Stall Force (N)	Static Hold Force (N)	Static Stiffness (N/m)	Preload on Stage (µm)	St Force Constant (mN/Command)
HR1	250	4	3.5	1	18	35
HR2	250	8	7	1.8	30	1.5
HR4	250	15	14	2.8	72	3
HR8	250	30	28	3.8	144	6

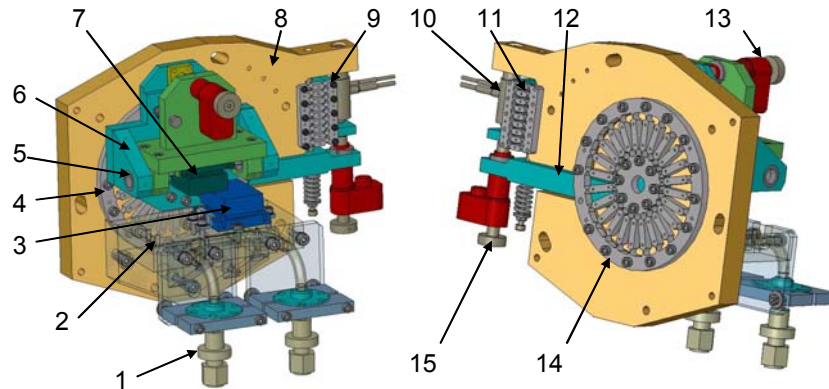
Note: All motor performance data is based on using Nanomotion c-series, motors and amplifiers.



Courtesy of Nanomotion Inc.



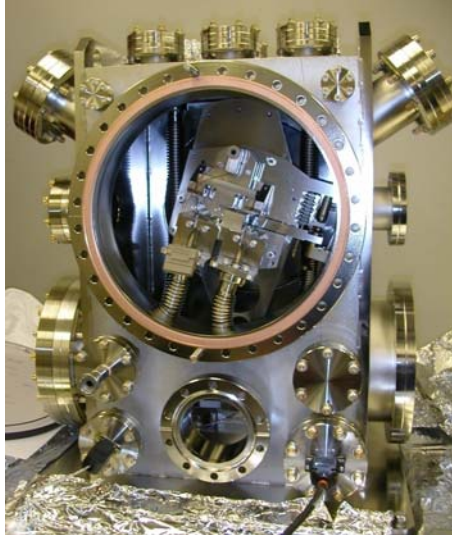
## UHV-Compatible Artificial Channel-Cut Crystal Mechanism



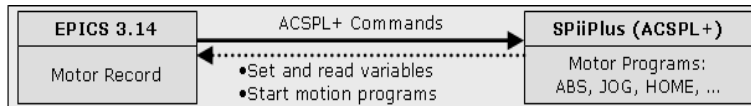
Front side and back side views of a 3-D model for a typical high-stiffness weak-link mechanism for an "artificial channel-cut crystal". (1) Cooling tube; (2) First crystal holder; (3) First crystal; (4) and (14) Rotary weak-link modules; (5) flexure bearing; (6) Second crystal holder; (7) Second crystal; (8) Base plate; (9) and (11) linear weak-link modules; (10) PZT actuator; (12) Sine bar; (13) and (15) Picomotor™ actuators. [9]



### UHV-Compatible Artificial Channel-Cut Crystal Mechanism



### Monochromator Control System



• An important control requirement was ensuring that this new monochromator sine bar driver assembly could be seamlessly integrated into Beamline 8-ID's VME-based-EPICS beamline control system.

• This was completed by creation of an EPICS 3.14 device driver so that a standard EPICS motor record can communicate over Ethernet with ACSPL+ command sequences exposed by a socket layer hosted on the ACS Motion™ SPiiPlus motion controller.

• Aside from allowing us to integrate this motion into our control system, the Ethernet-based architecture permits ready access to specialized servo tuning, motion-profile-creation, ..., using ACS Motion's™ SPiiPlus MMI Windows™-based application without switching delicate cabling. [8]

### Test Results and Discussion

The new monochromator was installed in Beamline 8-ID-I in April 2006. [8]

**TABLE 1.** APS Beamline 8-ID-I Component Layout

Item	Distance from Radiation Source (m)
APS Undulator A	0.0
Windowless differential pump	25.0
0.3-mm diameter pinhole aperture	27.0
0.15° incident angle horizontal bounce plane Si mirror	29.1
0.1-micron root-mean-square (rms) surface finish Be window	33.0
Artificial channel cut monochromator	65.0
0.1-micron rms surface finish Be window	66.0
Collimating slits (wide open for the measurements presented in Fig. 1)	68.0
Exit flight path 75-micron-thick Kapton™ window	72.0
Roper Scientific CoolSnap HQ detector	72.5

### Test Results and Discussion

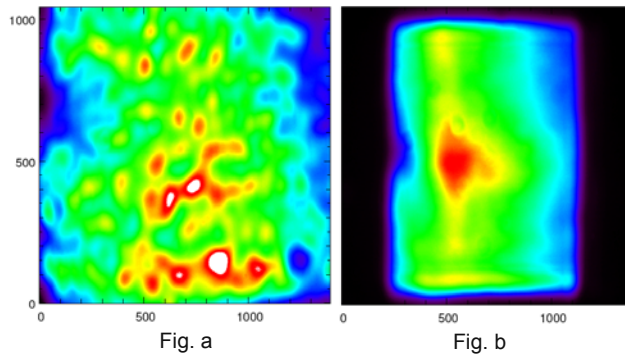
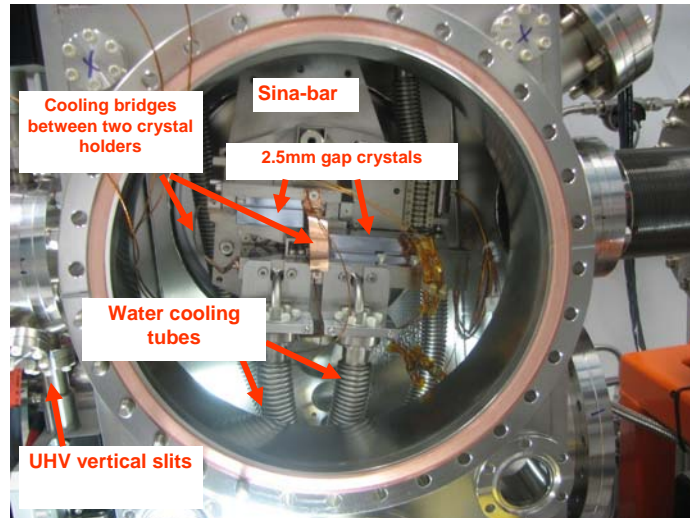


Fig. b shows the Ge(111)-monochromatized beam (7.35 keV) produced by the new monochromator. Evidently, its transverse intensity profile is considerably more uniform than that produced by the traditional channel-cut monochromator previously installed in Beamline 8-ID-I (Fig. a). In particular, the variance of the recorded intensities in the center range  $|X|$  and  $|Y| < 67$  microns is 50% less in Fig. (b) as compared to that in Fig. a. Moreover, the intensity in Fig. a varies rapidly over considerably smaller length scales versus that in Fig. b with negative implications for the stability of the overall set-up (since the smaller length scale (~ 25 micron) roughly corresponds in size to typical collimating apertures [1]). [8]

### UHV-Compatible Artificial Channel-Cut Crystal Monochromator for High Pressure Research



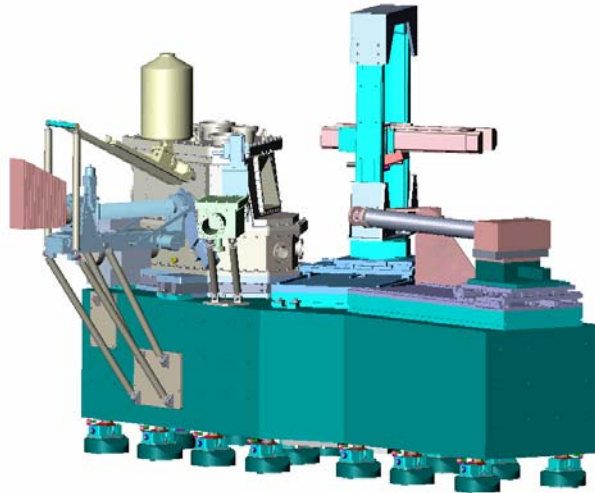
Courtesy of APS HP-CAT

### High-stiffness weak-link mechanism for linear motion reduction

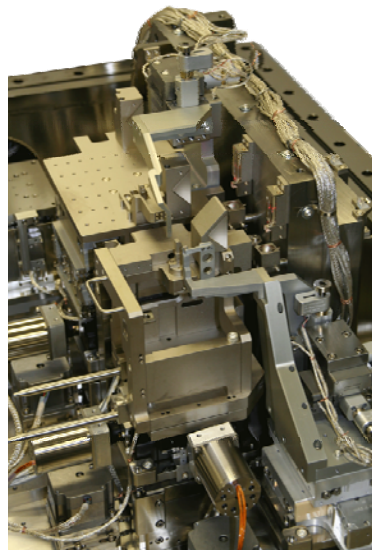


Using the same technique described in the section for the weak-link mechanism for a high-energy-resolution monochromator, we have developed a novel stage using a high-stiffness weak-link mechanism to perform linear motion closed-loop control at the **sub-100-pm** level with micron-level travel range. The structure consists of four groups of overconstrained weak-link parallelogram mechanisms made with lithography techniques. Driving sensitivity **better than 30 pm** was demonstrated with this weak-link linear-motion-reduction mechanism with a **1-micron travel range**.

*Introduction for ANL CNM nanoprobe project at APS*

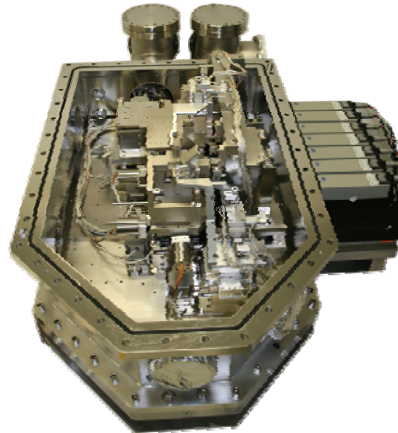
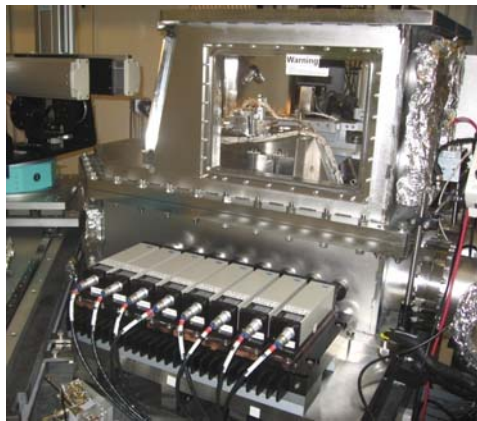


*Commissioning of the Argonne nanoprobe instrument*



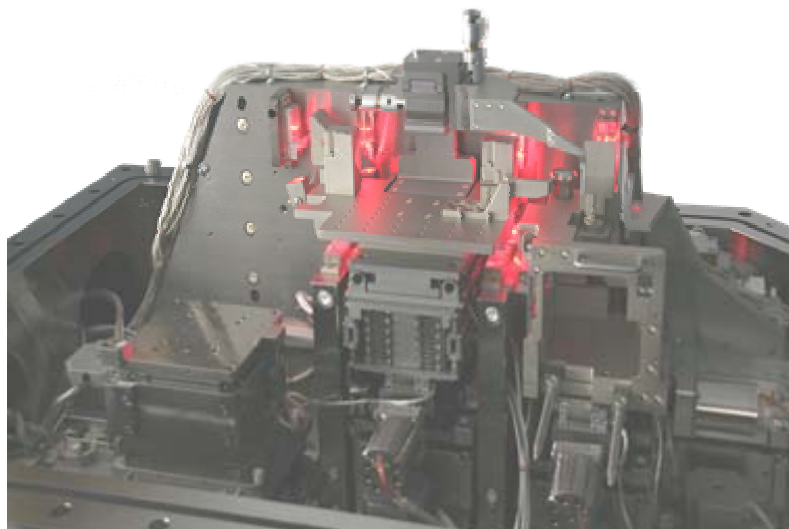
Courtesy of:  xradia

*Commissioning of the Argonne nanoprobe instrument*



Courtesy of:  xradia

*Commissioning of the Argonne nanoprobe instrument*



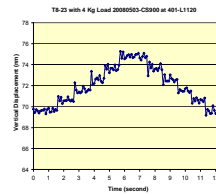
Courtesy of:  xradia

## Commissioning of the Argonne nanoprobe instrument



Courtesy of: 

## Commissioning of the Argonne nanoprobe instrument



A nanopositioning diagnostic setup has been built to support the CNM nanoprobe instrument commissioning process at the APS. Its laser Doppler interferometer system provides subnanometer positioning diagnostic resolution with large dynamic range. A set of original APS designed ultraprecision PZT-driven weak-link stages with high stiffness motor-driven stages has been tested with this diagnostic setup.

## Summary

More than forty sets of rotary laminar weak-link mechanisms have been made for APS users in synchrotron radiation instrumentation applications, such as high-energy-resolution monochromators for inelastic x-ray scattering, UHV-compatible monochromator for XPCS, and x-ray analyzers for ultra-small-angle scattering, and powder-diffraction experiments. Linear laminar weak-link mechanisms also demonstrated high resolution with high stiffness for high-precision linear stage applications, such as x-ray nanoprobe applications.

Commercial available now.

## Acknowledgments

The authors would like to thank D. Nocher, and R. Ranay from the Argonne National Laboratory for their help in the development of laminar weak-link mechanisms . This work was supported by the U.S. Department of Energy, Office of Science, under Contract No. DE-AC02-06CH11357.

## References

- [1] T. S. Toellner, T. Mooney, S. Shastri, and E. E. Alp, SPIE Proc. vol. 1740 (1992) pp. 218.
- [2] E. E. Alp et al., Hyperfine Interactions 90 (1994) pp. 323.
- [3] D. Shu, Y. Han, T. S. Toellner, and E. E. Alp, Proc. SPIE, Vol. 4771 (2002) 78-90
- [4] D. Shu, E. E. Alp, J. Barraza, and T. M. Kuzay, Proc. SPIE, Vol. 3429 (1998) 284-292
- [5] U.S. Patent granted No. 6,607,840, D. Shu, T. S. Toellner, and E. E. Alp, 2003
- [6] LDDM is a trademark of the Optodyne Inc., 1180 Mahalo Place, Compton, CA 90220, U.S.A.
- [7] D. Shu, T. S. Toellner, and E. E. Alp, Nucl. Instrum. and Methods A 467-468, 771-774 (2001)
- [8] Instruction manual, Physik Instrumente GmbH & Co., Germany, 2003
- [9] Picomotor is a trademark of Newfocus Co., California
- [10] D. Shu et al., MEDSI 2002, APS, Chicago, U.S.A., 2002
- [11] D. Shu, MEDSI 2004, ESRF, Grenoble, France, 2004
- [12] T. S. Toellner, APS Science 2004, ANL-05/04, p. 130
- [13] S. Narayanan et al., SRI-2006 Conf. Proc. 879, AIP (2007) 911-914.
- [14] Y. Zhang, A. P. Wilkinson, P. L. Lee, S. D. Shastri, D. Shu, D. -Y. Chung, M. G. Kanatzidis, J. Appl. Cryst. 38, 433-441 (2005).
- [15] B. Jakobsen, H. F. Poulsen, U. Lienert, J. Almer, S. D. Shastri, H. Sorensen, C. Gundlach, W. Pantleon, Science 312, 889-892 (2006).
- [16] J. Ilavsky et al., SRI-2006 Conf. Proc. 879, AIP (2007) 1833-1836.
- [17] P. Lee, M. A. Beno, D. Shu, M. Ramanathan, J. F. Mitchell, J. D. Jorgensen, and R. B. Von Dreele, SRI 2003 Conf. Proc. 705, AIP (2004) 388-391.
- [18] U.S. Patent granted No. 5,896,200, D. Shu, 1999
- [19] U.S. Patent granted No. 6,822,733, D. Shu, 2004.
- [20] D. Shu et al., SRI-2006 Conf. Proc. 879, AIP (2007) 1073-1076.
- [21] D. Shu et al., SRI-2006 Conf. Proc. 879, AIP (2007) 1321-1324.
- [22] Catalog and exhibition, Xradia, Inc., Concord, CA 94520, 2008
- [23] U.S. Patent granted No. 6,984,335, D. Shu, T. S. Toellner, and E. E. Alp, 2006
- [24] U.S. Patent granted No. 7,162,888, D. Shu, A. Joachimiak, C. Preissner, D. Nocher, Y. Han, J. Barraza, P. Lee, W. Lee, Z. Cai, S. Ginell, R. Alkire, R. Schuessler, 2007
- [25] U.S. Patent granted No. 7,331,714, D. Shu, J. Maser, B. Lai, S. Vogt, M. Holt, C. Preissner, R. Winarski, G. Stephenson, 2008